AIP | Applied Physics Letters

Ultraviolet-enhanced room-temperature gas sensing by using floccule-like zinc oxide nanostructures

Yu-Hsuan Ho, Wen-Sheng Huang, Hao-Chun Chang, Pei-Kuen Wei, Horn-Jiunn Sheen, and Wei-Cheng Tian

Citation: Applied Physics Letters **106**, 183103 (2015); doi: 10.1063/1.4919921
View online: http://dx.doi.org/10.1063/1.4919921
View Table of Contents: http://scitation.aip.org/content/aip/journal/apl/106/18?ver=pdfcov
Published by the AIP Publishing

Ultraviolet-enhanced room-temperature gas sensing by using floccule-like zinc oxide nanostructures

Yu-Hsuan Ho,[1,2] Wen-Sheng Huang,[1] Hao-Chun Chang,[3] Pei-Kuen Wei,[2] Horn-Jiunn Sheen,[3,a)] and Wei-Cheng Tian[1,a)]
[1]*Graduate Institute of Electronics Engineering, National Taiwan University, Taipei 10617, Taiwan*
[2]*Research Center for Applied Sciences, Academia Sinica, Taipei 115, Taiwan*
[3]*Institute of Applied Mechanics, National Taiwan University, Taipei 10617, Taiwan*

(Received 16 December 2014; accepted 28 April 2015; published online 4 May 2015)

The self-aggregation of floccule-like ZnO nanostructures that were shaped by an anodic aluminum oxidation (AAO) template to improve photoactivation and sensing performance was demonstrated. Because of differences in the surface energy between the densely distributed nanopores of AAO templates, sputtered ZnO materials were located in constricted regions and aggregated into roughened nanostructures with a high surface-to-volume ratio. Because of the generation of oxygen ions by ultraviolet illumination, the room-temperature-sensing responses showed a high degree of linearity with a resistance variation of 1.758% per 100 ppm of octane gas. The optimized sensing performance of the self-organized ZnO nanostructures was increased and was 15.4 times higher than that of an unpatterned ZnO thin film. © *2015 AIP Publishing LLC*.
[http://dx.doi.org/10.1063/1.4919921]

Volatile organic compound (VOC) sensors have been used in a wide range of industries, such as the chemical, biomedical, and food industries, and for ambient air monitoring.[1,2] Considerable research effort has been devoted in developing functional materials, such as metal oxides, polymers, and other nanomaterials, which may be used for constructing high-performance VOC vapor sensors.[3–5] Among these materials, nanostructured metal-oxide-based sensors have attracted considerable attention, primarily because of their low cost, production flexibility, high reliability, multiple-gas detection capability, and potential integrability with complementary metal-oxide semiconductors or microelectromechanical systems.[6–8] Most previous studies have focused on ZnO, SnO_2, ZrO_2, CuO, and WO_3 nanostructures with high surface-to-volume ratios.[9] Thermal activation is the most widely used method for providing sufficient energy for gas sensing.[6] However, the necessity of using high operation temperatures restricts the sensor applicability; for example, this necessity affects their use as portable devices, in low power consumption applications, and for monitoring explosive gas species. Recently, many approaches involving the use of light irradiation to activate surface reactions have been proposed for overcoming these drawbacks.[10–12] Nanostructured metal oxide materials not only increase the surface-to-volume ratio, which improves the sensing capability, but also enhance light absorption, improving photoactivated sensing responses. Recently, many metal oxide nanostructures such as nanorods,[13,14] nanowires,[15,16] and nanopores[17] have been designed and fabricated, and they have shown good gas sensing characteristics. Their use in high-performance VOC sensing is impeded by the challenges posed by their complex fabrication process. Anodic aluminum oxidation (AAO) is a conventional and reliable technique for nanostructure fabrication. In this study, we fabricated floccule-like ZnO nanostructures by using an AAO template to enhance room-temperature sensing performance and analyzed their growth mechanisms.

The process for fabricating the floccule-like ZnO nanostructures is shown in Fig. 1. ZnO materials were perpendicularly deposited on AAO templates through magnetron sputtering at room temperature, with a deposition rate of approximately 0.3 nm/min and a sputtering pressure of approximately 5×10^{-3} Torr. The distance between the target and the AAO template was approximately 5 cm. Before deposition, surface defects on the AAO templates were removed through Ar^+ ion bombardment. AAO template surfaces were used as the nucleation and growth sites for the formation of floccule-like ZnO nanostructures.

Figure 2 shows plane-view SEM images of ZnO sputtered on a patterned AAO template and a flat thermally

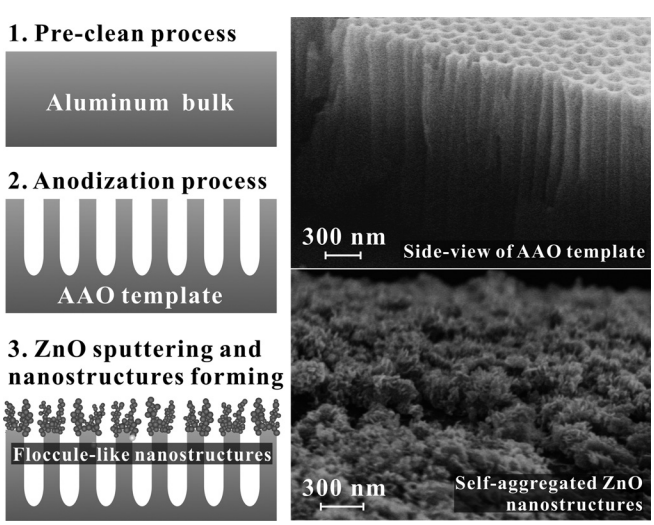

FIG. 1. Diagrams of fabrication process and SEM images of the self-aggregated floccule-like ZnO nanostructures.

a)Electronic addresses: sheenh@ntu.edu.tw and wctian@cc.ee.ntu.edu.tw. Tel.: + 886-2-3366-9852. Fax: + 886-2-2367-1909.

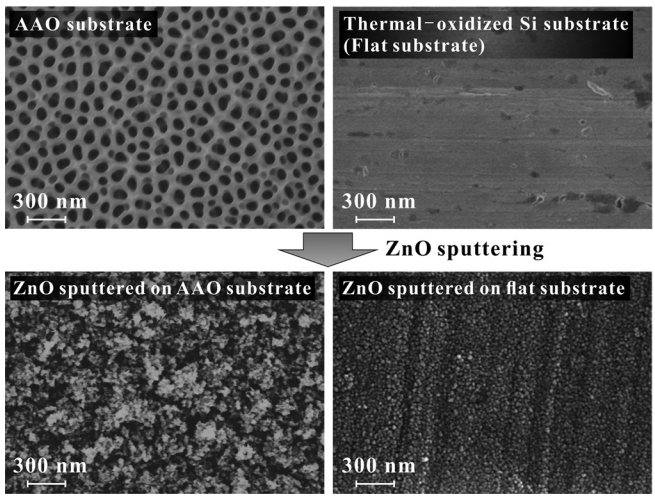

FIG. 2. Surface morphology of ZnO sputtered on the nanoporous AAO template and flat thermal-oxidized aluminum substrate.

oxidized aluminum substrate. After ZnO deposition, almost all of the ZnO atoms formed stacks in the interpore regions of the AAO templates, unlike the formation of continuous films on a flat silicon/silicon dioxide wafer. Specific surface regions (corner regions) are the nucleation sites for ZnO grains, which proceed to grow into floccule-like nanostructures. The growth mechanism of the nanostructures on the surfaces of AAO templates is attributed to the surface effect of high surface-to-volume ratios described in Refs. 18–20. To understand the growth process of the floccule-like ZnO nanostructures, SEM images of ZnO sputtered on a patterned AAO template at different times are shown in Fig. 3. Initially, most of the nucleation occurs heterogeneously at free surfaces, especially at edges or defects. These are regions of high surface free energy, and excess energy is available for material nucleation. Therefore, to reduce the surface free energy, heterogeneous nucleation occurs at the edges or defects. ZnO clusters apparently nucleated and grew around the pores, as shown in the SEM images of Fig. 3. All nucleation sites were conjointly formed. Furthermore, the deposited ZnO tended to be stacked upward and caused the nanostructures to be stretched and crossed to

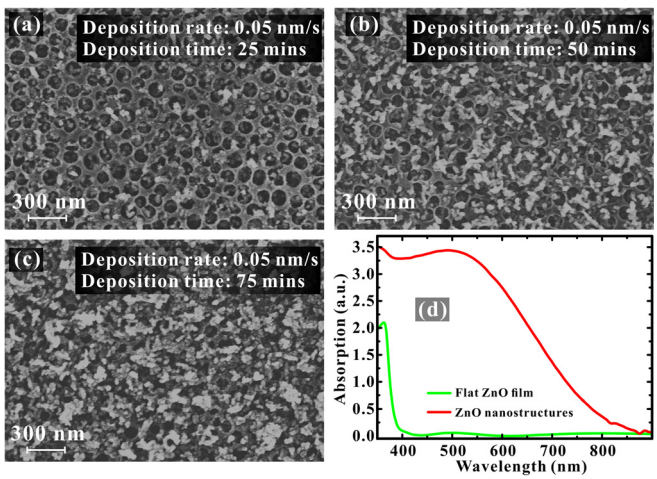

FIG. 3. (a)–(c) SEM images of ZnO sputtered on the patterned AAO template with constant deposition rate (0.3 nm/min) and different deposition time; (d) absorption spectra of the floccule-like ZnO nanostructures.

form floccule-like ZnO nanostructures. Complex nanostructures could show increased light-trapping effects and light absorption.[21] Figure 3(d) shows absorption spectra of the ZnO sputtered on the flat substrate and AAO substrate. The peak absorption of the flat ZnO film was at 363 nm (~3.4 eV) with an absorption edge at 389 nm (~3.19 eV). The flat ZnO film had almost no absorption in the wavelength range of visible light. However, because of the strong light-trapping effects of the floccule-like ZnO nanostructures, the optical extinction was extended to the range of visible light. The intrinsic ultraviolet (UV) absorption at the wavelength of 363 nm also exhibited substantial improvement, which can be expected to enhance photoactivation for gas sensing.

To examine the effect of the pore diameter and interpore size of AAO templates on the growth mechanism of ZnO, three types of AAO templates with pore diameters of approximately 53, 84, and 111 nm were used. All of the samples were sputtered at a deposition rate of 0.3 nm/min for 75 min and annealed at 500 °C for 1 h. The results are shown in Fig. 4. The sheet resistance of ZnO sputtered on the flat surface was approximately 2.27 kΩ/□. For the AAO templates with a pore diameter of 53 nm, the sputtered ZnO materials aggregated to form a rough surface, as shown in Fig. 4(a), and, consequently, the sheet resistance increased to 2.5 MΩ/□. When the ZnO materials were sputtered on the AAO templates with a pore diameter of 84 nm, floccule-like ZnO nanostructures were formed, and the sheet resistance was

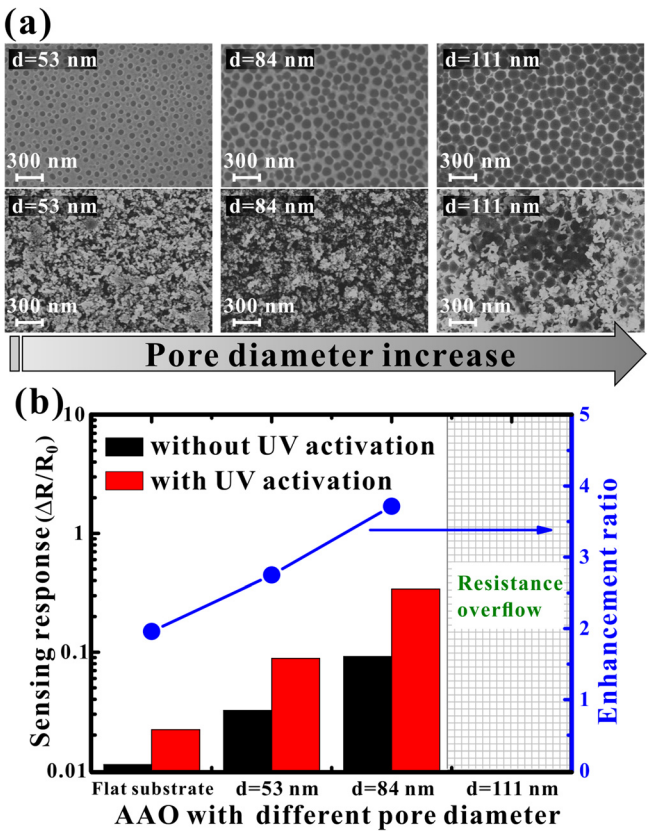

FIG. 4. Surface morphology (a). Sensing responses (b) of ZnO sputtered on the patterned AAO template with different pore diameter and interpore size (deposition rate: 0.3 nm/min; deposition time: 75 min; target gas: octane, 5000 ppm).

approximately 4.64 MΩ/□. The nanostructured ZnO films can be expected to have a high surface-to-volume ratio and favorable sensing performance. For the AAO templates with a pore diameter of 111 nm, ZnO clusters nucleated, but the subsequent growth of the material was restricted. A discontinuous ZnO film on the AAO substrate is shown in Fig. 4(a). The sheet resistance could not be measured in this case. Fig. 4(b) shows the sensing response of the proposed sample upon exposure to octane at a concentration of 5000 ppm. As the pore size increased, more porous ZnO nanostructures, which could show stronger sensing responses, formed. In addition, the porous nanostructures were beneficial for light trapping and the photoactivation of room-temperature gas sensing. For the AAO template with a pore diameter of 84 nm, the sensing response for 5000 ppm of octane gas increased by a factor of 3.72 upon UV activation.

The transient responses of the optimized ZnO nanostructures (pore size: 84 nm; deposition time: 75 min) to octane gas with and without UV activation at room temperature are shown in Fig. 5(a). The prepared ZnO nanostructures are tested using a four-point probe and gas injection system, in which ambient air, filtered by the trapper, was pumped through an air compressor and was mixed with octane gas to form various concentrations for the ZnO nanostructures characterizations. For short-wavelength UV irradiation, more electrons were generated on the surface of ZnO, and the initial sheet resistance decreased sharply from 4.6 to 2.2 MΩ because of an increase in the number of free carriers. The mechanism of metal oxide sensing at room temperature was markedly different from that at a high temperature. The photoactivated oxygen ions on the ZnO surface reacted with the gas molecules. This oxidization resulted in a decrease in the number of oxygen ions on the surface and an increase in the number of free electrons on the ZnO surface. This increase in the number of free electrons in the ZnO material increased the equivalent conductance of the ZnO nanostructures. The increase in the number of electrons also enhanced the oxidization of the surface organic contaminant; thus, the surface of the sensing layer was cleaned, enhancing gas adsorption. Subsequently, additional photoinduced oxygen ions were generated, and this increased the number of binding sites for the target gas molecules. The influence of the octane concentration on the photoactivated gas sensing response ($\triangle R/R_0$) is shown in Fig. 5(b). The sensing response for UV activation shows a high degree of linearity with the resistance variation of 1.758% per 100 ppm of octane gas, which was higher than the resistance variation of the unpatterned ZnO film by a factor of 15.4.

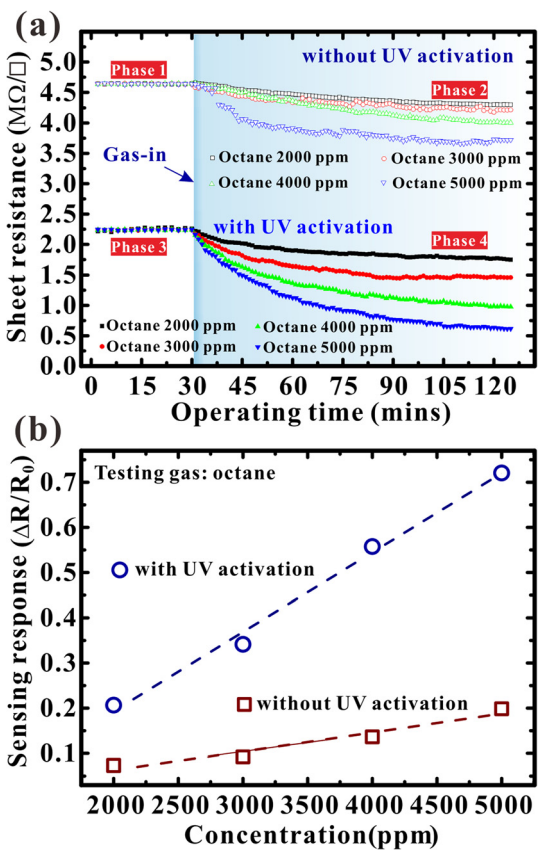

FIG. 5. Sheet resistance variation (a) and gas sensing response (b) of the floccule-like ZnO nanostructures exposed to octane gas with and without UV activation (phase 1: without octane injection and UV exposure; phase 2: with octane injection, without UV exposure; phase 3: without octane injection, with UV exposure; and phase 4: with octane injection and UV exposure).

In conclusion, this study demonstrated a convenient method for fabricating ZnO nanostructures with a high surface area and for achieving room-temperature VOC sensing under UV light activation. Floccule-like ZnO nanostructures were fabricated on the surface of a nanoporous AAO substrate. The rim of the pores, which act as obstacles to the stacked ZnO molecules, possibly prevented the molecules from forming continuous films. Moreover, the regions between closely distributed nanopores indicated insufficient surface energy for heterogeneous nucleation and restricted the growth of sputtered ZnO molecules. In these regions, instead of continuous films, complex nanostructures are formed. The use of UV light activation to form self-organized ZnO nanostructures was studied. Upon UV light irradiation, an appreciable number of UV-induced oxygen ions were generated on the ZnO surface, enhancing sensing response. A sensitivity of 1.76% per 100 ppm of octane gas was achieved; this sensitivity was 4.18 times higher than that of the ZnO nanostructures in the absence of UV light activation.

This research was supported by the National Science Council (Grant No. NSC-101-2627-E-002-005), Taiwan, and National Taiwan University (Contract No. 101R7624-2).

[1]C. L. Exstrom, J. R. Sowa, Jr., C. A. Daws, D. Janzen, K. R. Mann, G. A. Moore, and F. F. Stewart, Chem. Mater. **7**(1), 15 (1995).
[2]B. Timmer, W. Olthuis, and A. van den Berg, Sens. Actuators, B **107**(2), 666 (2005).
[3]W. C. Tian, Y. H. Ho, C. H. Chen, and C. Y. Kuo, Sensors (Basel) **13**(1), 865 (2013).
[4]Q. Fang, D. G. Chetwynd, J. A. Covington, C. S. Toh, and J. W. Gardner, Sens. Actuators, B **84**(1), 66 (2002).
[5]C. L. Li, Y. F. Chen, M. H. Liu, and C. J. Lu, Sens. Actuators, B **169**(0), 349 (2012).
[6]N. Barsan, D. Koziej, and U. Weimar, Sens. Actuators, B **121**(1), 18 (2007).
[7]M. E. Franke, T. J. Koplin, and U. Simon, Small **2**(1), 36 (2006).
[8]G. Korotcenkov, Mater. Sci. Eng., B **139**(1), 1 (2007).
[9]M. Gardon and J. M. Guilemany, J. Mater. Sci.: Mater. Electron. **24**(5), 1410 (2013).

[10]E. Comini, G. Faglia, and G. Sberveglieri, *Solid State Gas Sensing* (Springer, 2009).
[11]S. W. Fan, A. K. Srivastava, and V. P. Dravid, Appl. Phys. Lett. **95**(14), 142106 (2009).
[12]W. C. Tian, Y. H. Ho, and C. H. Chou, IEEE Sens. J. **13**(5), 1725 (2013).
[13]O. Lupan, G. Chai, and L. Chow, Microelectron. Eng. **85**(11), 2220 (2008).
[14]L. Wang, Y. Kang, X. Liu, S. Zhang, W. Huang, and S. Wang, Sens. Actuators, B **162**(1), 237 (2012).
[15]Q. Wan, Q. H. Li, Y. J. Chen, T. H. Wang, X. L. He, J. P. Li, and C. L. Lin, Appl. Phys. Lett. **84**(18), 3654 (2004).
[16]G. Zheng, F. Patolsky, Yi. Cui, W. U. Wang, and C. M. Lieber, Nat. Biotechnol. **23**(10), 1294 (2005).
[17]S. E. Lewis, J. R. DeBoer, J. L. Gole, and P. J. Hesketh, Sens. Actuators, B **110**(1), 54 (2005).
[18]C. Y. Kuo, S. Y. Lu, and T. Y. Wei, J. Cryst. Growth **285**(3), 400 (2005).
[19]X. M. Li, K. Dong, L. B. Tang, Y. J. Wu, P. Z. Yang, and P. X. Zhang, Appl. Surf. Sci. **256**(9), 2856 (2010).
[20]K. T. Huang, P. C. Kuo, G. P. Lin, C. L. Shen, and Y. D. Yao, Thin Solid Films **518**(18), 5300 (2010).
[21]E. Yablonovitch and G. D. Cody, IEEE Trans. Electron Devices **29**(2), 300 (1982).